Quest Journals
Journal of Electronics and Communication Engineering Research
Volume 10 ~ Issue 3 (2024) pp: 09-18
ISSN(Online) : 2321-5941
www.questjournals.org

Research Paper

Relationship Between Impedance Transition Point and Cell Wall in Plant Tissue

Koyu Chinen[1], Shoko Nakamoto[2], Ichiko Kinjo[3]
[1,2](GLEX, Yokohama, Japan)
[3](Information and Communication Eng. Dept., National Institute of Technology, Okinawa College, Japan)

ABSTRACT: *The impedance calculated from the S-parameters measured for fifteenplant varieties showed a transition point of variation that increased or decreased the reactance at a frequency of 1 to 100MHz. This transition point varied according to the plant variety. In the synthesized equivalent circuit, the series circuit changed to a parallel circuit after the transition point when the frequency was increased. The transition point disappeared when the plant samples were grated and filtered. The transition point was found to be related to the equivalent circuit of the plant cell wall.*

KEYWORDS: *S-parameter,Bioimpedance,Plant-tissue equivalent circuit,Cell wall, Fruit and vegetable*

R*eceived 05 Mar., 2024;* ***R****evised 16 Mar., 2024;* ***A****ccepted 18 Mar., 2024* © *The author(s) 2024.*
P*ublished with open access at* ***www.questjournals.org***

I. INTRODUCTION

By measuring the electrical characteristics of plant cells, it is possible to classify plant varieties, analyze growth conditions, determine ripening conditions, and analyze cellular organization. Furthermore, by representing the cellular tissue as an equivalent electrical circuit, it is possible to perform collaborative analysis by applying high-frequency circuit measurement technology and simulators [1]-[9]. In this study, we measured the scattering parameter S_{11} using a portable vector network analyzer (VNA) and a miniature SMA (sub-miniature type A) probe. We synthesized an equivalent circuit by curve-fitting the impedance curve on a Smith chart. In addition, we observed a transition point in the frequency variation of the measured impedance Z_{in}, where the mode of change changed significantly. This paper focuses on this transition point and analyzes the equivalent circuit of plant cells.

II. S-PARAMETER MEASUREMENTS ON PLANT SAMPLES USING A PORTABLE VNA AND SMA PROBE

The S-parameter measurement system for the plant samples is shown in Figure 1. The S-parameter reflection coefficient S_{11} was measured in the 1-100 MHz frequency range using a portable vector network analyzer equipped with an SMA probe. The input impedance Z_{in} was calculated from the measured S-parameter S_{11}. The SOLT (short, open, load, through) SMA connector was used to calibrate the measurement system. The calibration was verified by measuring and comparing the resistance of a 1608 (mm) size 1200 Ω SMD (surface mount device) soldered between the signal and ground pins of the measurement SMA probe (Figure 2). It consists of three pins: a central signal pin (gold-plated copper, 4 mm × ϕ 0.8 mm) surrounded by PTFE (polytetrafluoroethylene) and two ground pins (gold-plated brass, 4 mm × ϕ 0.8 mm) on either side, spaced 4 mm apart. A cross-sectional view of the SMA probe inserted into the plant sample is shown in Figure 3. The number of measurement points on the plant sample surface was approximately 10, and the average value of the reflection coefficient S_{11} of the S-parameters measured at each point was determined. The SMA probe is simpler and smaller than the impedance analyzer instrument [10]. It, therefore, allows non-invasive measurements on legumes and plants with uneven surfaces and field measurements without processing.

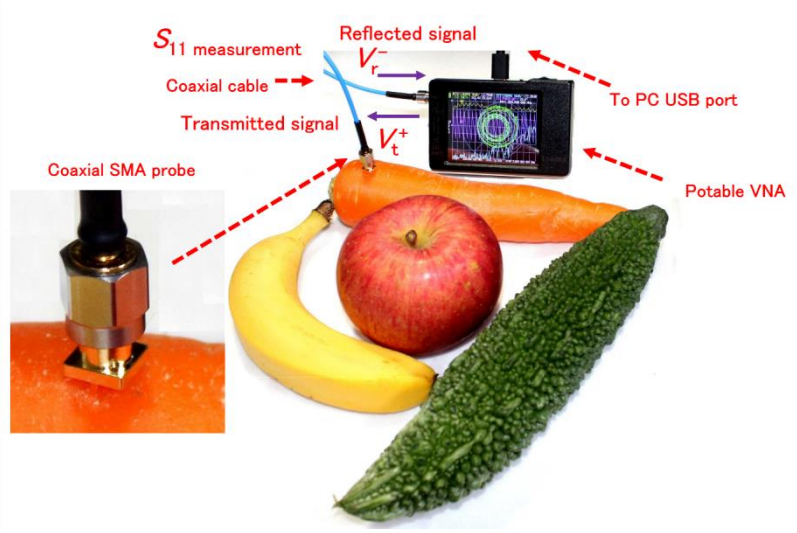

Figure1: Configuration of the S-parameter S_{11} measurement setup for plants using a portable VNA with a tiny SMA probe.

III. CALCULATION OF S-PARAMETER S11 AND IMPEDANCE ZIN BY TRANSMISSION CIRCUIT MODEL

The circuit model for measuring the S-parameter S_{11} of the sample (DUT) by VNA and calculating the impedance is shown in Figure 4, where the reflection coefficient of S_{11} is expressed as $S_{11} = b_1 / a_1$ using the normalized voltage a_n, $b_n = V_n/\sqrt{Z_0}$. The impedance $Z(x)$at point x is expressed by equation (1) using the traveling wave voltage $A\varepsilon^{-\gamma x}$, the reflected wave voltage $B\varepsilon^{\gamma x}$, and the S-parameter reflection coefficient $S_{11}(x)$ at point x. Since $S_{11}(x)$ is expressed as a complex number, the input impedance Z_{in} of the measurement sample can be represented by equations (2) and (3), where Z_0 is the characteristic impedance (50Ω) and γ is the propagation coefficient.

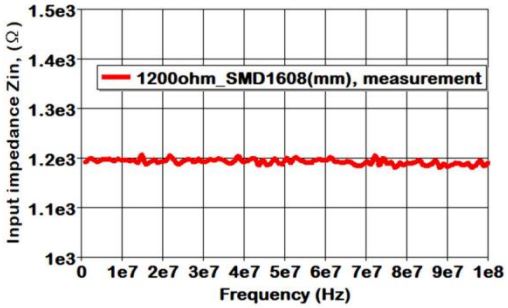

Figure2: Impedance Z_{in} calculated from the S-parameter S_{11} measurement of a surface-mount resistive device (1200 Ω) using the SMA probe

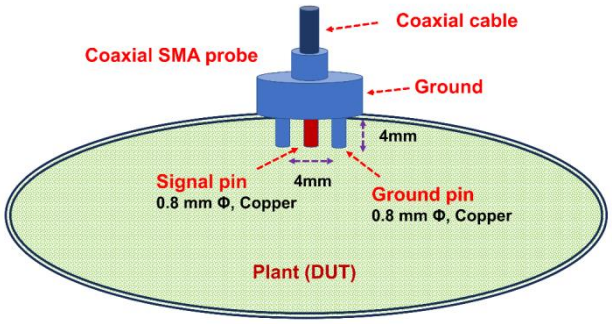

Figure3: Cross section of the SMA probe inserted into the plant sample

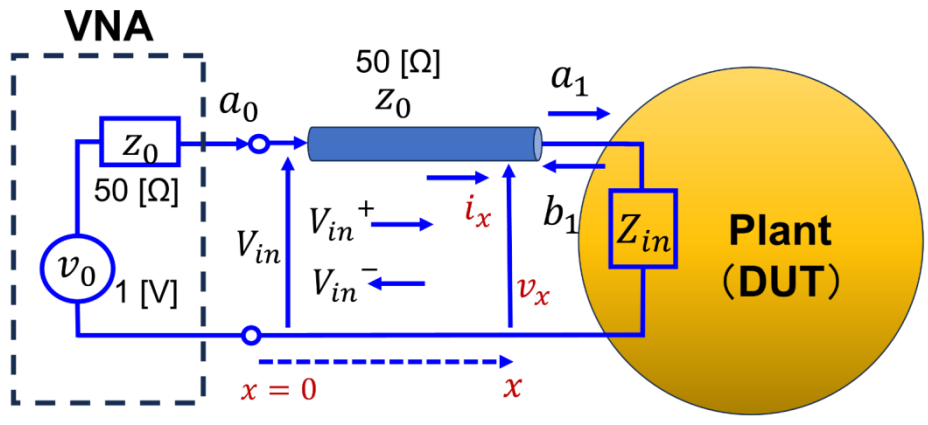

Figure4: Impedance Z_{in} calculated from the S-parameter S_{11} measurement

$$Z(x) = \frac{V_{in}(x)}{-I_{in}(x)} = Z_0 \frac{A\varepsilon^{\gamma x} + B\varepsilon^{-\gamma x}}{A\varepsilon^{\gamma x} - B\varepsilon^{-\gamma x}} = Z_0 \frac{1 + S_{11}(x)}{1 - S_{11}(x)} \tag{1}$$

$$Z_{in} = Z_0 \frac{\sqrt{[1 + S_{11}(Re)]^2 + [S_{11}(Im)]^2}}{\sqrt{[1 - S_{11}(Re)]^2 + [S_{11}(Im)]^2}} \varepsilon^{j(\theta_1 - \theta_2)} \tag{2}$$

$$\theta_1 = \tan^{-1} \frac{-S_{11}(Im)}{1 - S_{11}(Re)} \quad , \quad \theta_2 = \tan^{-1} \frac{S_{11}(Im)}{1 + S_{11}(Re)} \tag{3}$$

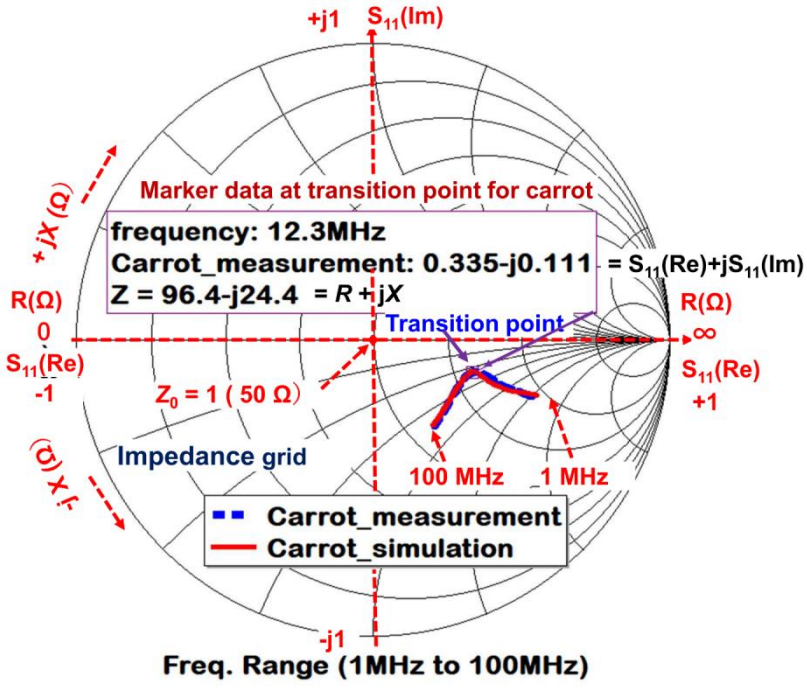

Figure5: Measured and simulated Z_{in} impedance values plotted on the impedance grid of a Smith chart

IV. EQUIVALENT CIRCUIT OF A PLANT CELL DEDUCED FROM IMPEDANCE ZIN

We calculated the input impedance Z_{in} from the S-parameter S_{11} measured using the measurement system in Figure 1 and plotted it on the impedance grid of the Smith chart. The results are shown in Figure 5. The sample used for the measurement was a carrot. The measured S-parameter S_{11} values were analyzed using RF circuit simulators (QucsStudio and AWR-MWO) [11], [12], and an equivalent circuit was synthesized by curve fitting the impedance Z_{in} calculated from S-parameter S_{11} on a Smith chart. Plant cells consist mainly of intracellular tissues surrounded by cell membranes and walls, as shown in Figure 6 [4], [19]. In the case of plants, most of the intracellular tissue is occupied by vacuoles. Based on the impedance Z_{in} trajectory on the Smith chart and the plant cell structure, the equivalent circuit of a plant cell is considered to be a parallel circuit of multiple C_nR_n series branches circuits, and the synthesized equivalent circuit, S parameters, and simulation conditions are shown in Figure 7. Since elements C_1 and R_1 are associated with the vacuole, C_2 and R_2 with the cytoplasm, C_3 and R_3 with the plasma membrane, and C_4 and R_4 with the cell wall, the equivalent circuit consists of Y_1, Y_2, Y_3, and Y_4 in parallel.

From the S-parameter simulation of this equivalent circuit, the input impedance Z_{in} and the admittance Y_{in} were calculated; since Z_{in} and Y_{in} are expressed in complex numbers, the resistance R and the reactance jX, the conductance G and the susceptance jBwere calculated, respectively. The input impedance Z_{in}, obtained from the measured complex S-parameter S11, is also expressed in complex numbers, as shown in equation (2), so R, j$X$and G, jB can be calculated. The measured Z_{in}, R, jX, Yin, G, jB, and simulated values are shown in Figure 8 and Figure 9, respectively. The measured and simulated values are solid and dashed lines, respectively. The measured and simulated values almost overlap, and the equivalent circuit in Figure 7 represents the plant cell structure shown in Figure 6. Among plant cells, the cell wall plays an essential role in plant function and has been the subject of various studies [10], [15]-[22].

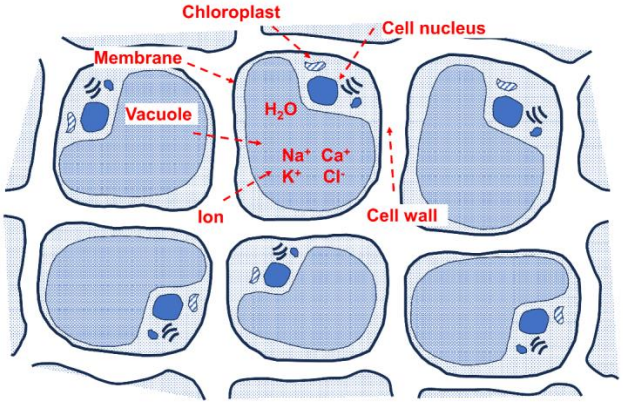

Figure6: Structures of a plant cell's vacuole, cytoplasm, and membrane wall

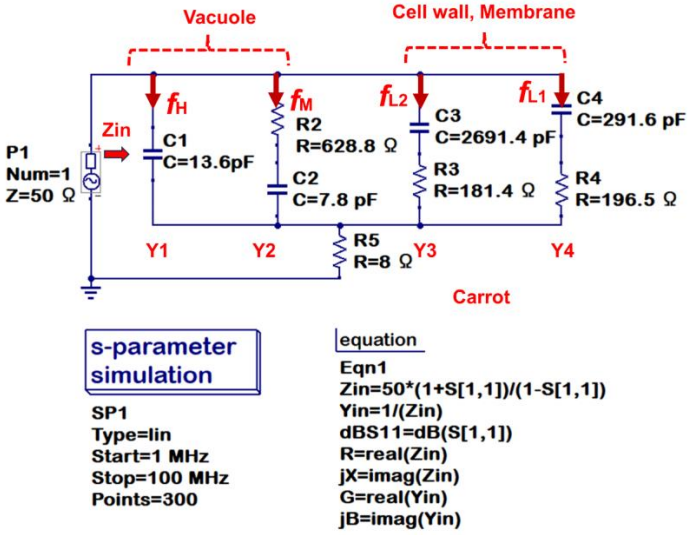

Figure7: Equivalent circuit model of a plant cell and S-parameter

V. TRANSITION POINT OF IMPEDANCE IN PLANT CELLS

The measured and simulated values of the input impedance Z_{in} on the Smith chart shown in Figure 5 also almost overlap. The curve of input impedance Z_{in} shows a significant transition point at a certain frequency; as the frequency is increased from 1 MHz, the curve shows the path of a series *CR* circuit up to the transition point, but from the transition point to 100 MHz, the curve follows the parallel *CR* circuit. From the transition point to 100 MHz, the curve trajectory is along the admittance grid, representing a parallel *CR* circuit.

In the frequency variation of the measured and simulated impedance Z_{in}, resistance *R*, and reactance j*X* shown in Figure 8, a transition point appears in the reactance j*X*curve that changes from increasing to decreasing. The frequency of this transition point is 12.3 MHz, the same frequency as the transition point of the input impedance Z_{in} on the Smith chart shown in Figure 5.In the frequency variation of the measured and simulated values of admittance Y_{in}, conductance *G*, and susceptance j*B* shown in Figure 9, a transition point appears in the susceptance j*B* curve that changes from decreasing to increasing. The frequency of this transition point is 12.3 MHz, the same frequency as the transition point of the input impedance Z_{in} on the Smith chart. After the transition point of impedance Z_{in}, the equivalent circuit changes from a series circuit to a parallel circuit.

Figure 10 shows a model of the structure of a plant cell and the transmission paths for high-frequency signals (1 to 100 MHz). The cell wall consists mainly of cellulose. Cellulose is a dielectric with high electrical resistance R_4, forming a capacitor C_4 between the cellulose cells. The low-frequency signal f_{L1} propagates mainly along the Y_4 path of C_4 and R_4 because it passes through the cell wall. The low-frequency signal f_{L2} has a slightly higher frequency than f_{L1} and propagates mainly along the Y_3 path of C_3 and R_3, which represents the cell membrane. The intermediate frequency$f_M$propagates along the Y_2 path of C_2 and R_2, a cell wall and cytoplasm mixture. The vacuole contains dissolved ions such as Na^+ , Ca^+ , K^+ , Cl^-, and HPO^{2-}, which form a propagation path by ionic conduction, so the high-frequency signal f_H propagates along the Y_1 of C_1 in the vacuole.

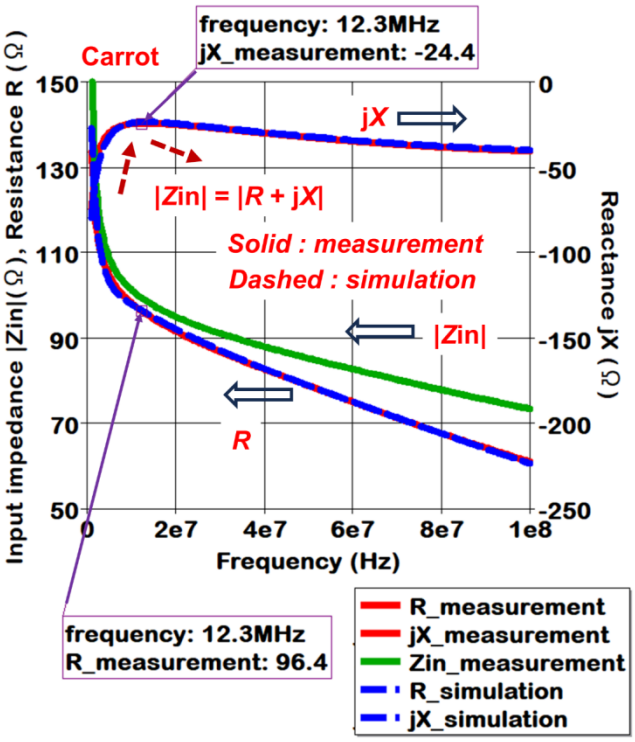

Figure8: Measured values and simulation results of impedance Z_{in}, resistance *R*, and reactance j*X*

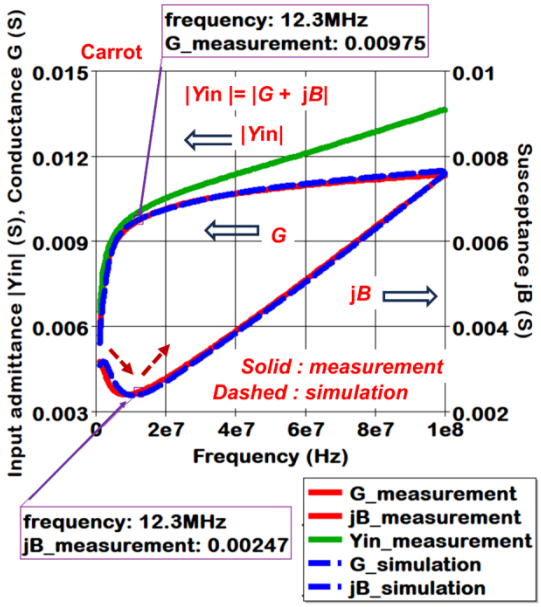

Figure9: Measured values and simulation results of admittance Y_{in}, conductance G, and susceptance jB

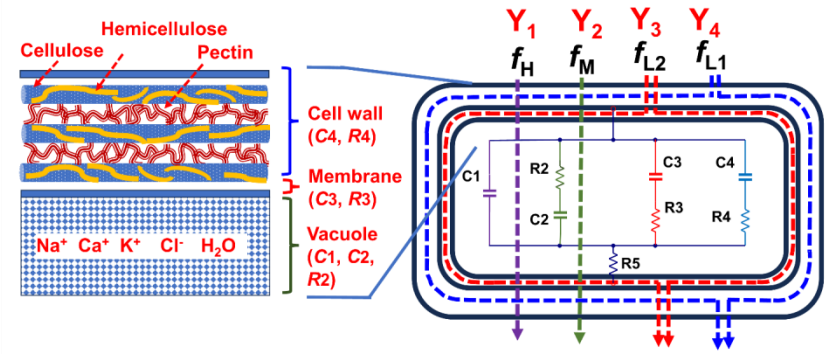

Figure10: Classification of high-frequency signals passing through the cell membrane, wall, cytoplasm, and vacuole of a plant cell

VI. IMPEDANCE ZIN MEASUREMENT AND EQUIVALENT CIRCUIT SYNTHESIS OF FIFTEEN FRUITS AND VEGETABLES

The values of the eight C_n, R_n, (n = 1-5) elements that comprise the equivalent circuit (Figure 7) synthesized from the impedance Zin and the admittance curves plotted on the Smith chart for the S-parameter S_{11} for the 15 fruit and vegetable samples are shown in Table 1. So-called vegetables and fruits have different transition points for the impedance Z_{in}. For example, as shown in Figure 11, the vegetable (carrot) has a higher frequency of the transition point, a more significant value of C_4, and a smaller resistance value of R_4. Fruits (peaches) have a low transition frequency, a low value of C_4, and a high resistance R_4.

In the equivalent circuit of a plant cell, the impedance Z_{34} of the parallel circuit of $Y_3 = 1/[R_3 - j/(\omega C_3)]$ and $Y_4 = 1/[R_4 - j/(\omega C_4)]$ can be calculated using Kirchhoff's law as follows.

$$|Z_{34}| = \frac{1}{\sqrt{\left[\sum_{n=3}^{4} \frac{\cos\theta_n}{\sqrt{{R_n}^2 + \frac{1}{(\omega C_n)^2}}}\right]^2 + \left[\sum_{n=3}^{4} \frac{\sin\theta_n}{\sqrt{{R_n}^2 + \frac{1}{(\omega C_n)^2}}}\right]^2}} \quad (4)$$

$$\theta_n = \tan^{-1}\frac{1}{\omega C_n R_n} \quad (5)$$

Table1: Values for each of the eight equivalent circuit elements extracted from the S-parameter S_{11} measurements for the fifteen plant species

Plants	C_1	R_2	C_2	C_3	R_3	C_4	R_4	R_5
Melon	22	780	0.2	1978	65	**9940**	**112**	15
Dragonfruit	17	747	7	1311	57	**3812**	**143**	16
Bananapeel	10	825	4	2981	101	**319**	**114**	4
Potato	14	410	16	4433	107	**257**	**209**	8
Whiteradish	13	5121	1	2196	168	**314**	**195**	8
Carrot	14	629	8	2691	181	**292**	**197**	8
Bananainner	12	1443	4	4436	186	**308**	**280**	8
Pineapple	12	45	1	4648	163	**60**	**802**	5
Cherry	11	736	6	1921	206	**99**	**534**	4
Onion	10	26	1	4120	268	**29**	**1236**	6
Mango	12	903	4	2164	302	**34**	**1107**	3
Grape	13	1366	9	2334	293	**24**	**2078**	8
Pear	8	97	2	1777	294	**4**	**1314**	2
Peach	13	1358	8	1878	314	**11**	**4204**	10
Unit	pF	Ω	pF	pF	Ω	pF	Ω	Ω

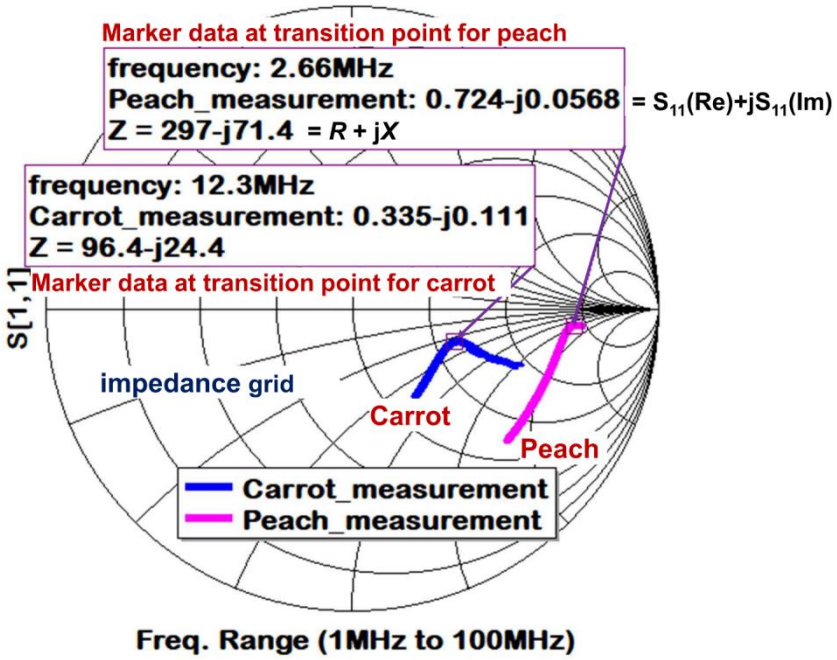

Figure11: Measured impedance Z_{in} of a vegetable (carrot) and a fruit (peach) plotted on a Smith chart

VII. TRANSITION POINTS AND EQUIVALENT CIRCUITS IN IMPEDANCE ZIN FOR FIFTEEN PLANT SAMPLES

The measured impedance Z_{in} at the transition points of the fifteenplant samples almost coincides with the calculated impedance Z_{34} of the equivalent circuit of Y_3 and Y_4 composed of C_3, R_3, C_4, and R_4 (Figure 12). It indicates that the transition point of the impedance Z_{in} is related to the electrical properties of the plant cell membrane and wall. The frequency of the transition point is inversely proportional to Z_{in} and Z_{34}. In addition, as shown in Figure 13, the measured impedance Z_{in} at the transition point almost coincides with the resistance R, and the reactance jX is inversely proportional to Z_{in} and R. The frequency of the transition point of the impedance Z_{in} is correlated with the change in the reactance jX.

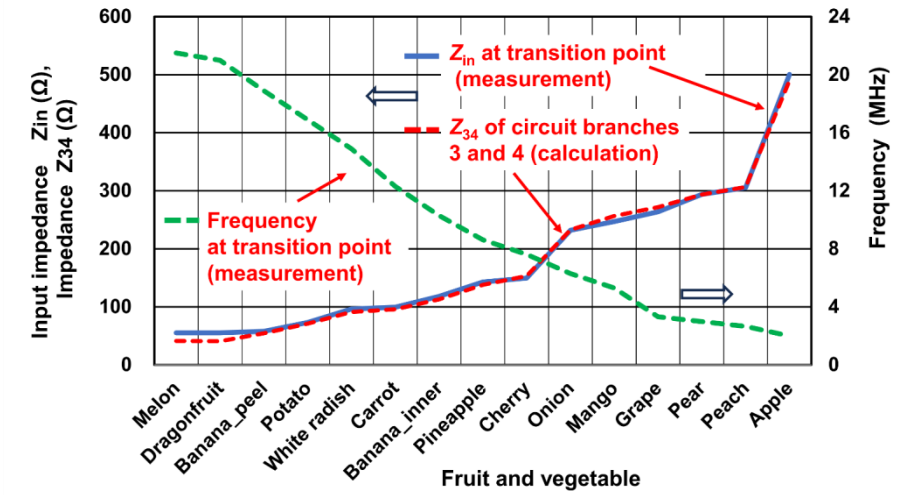

Figure12: Impedance Z_{in}, transition point impedance Z_{34}, and frequency for fifteenplant species

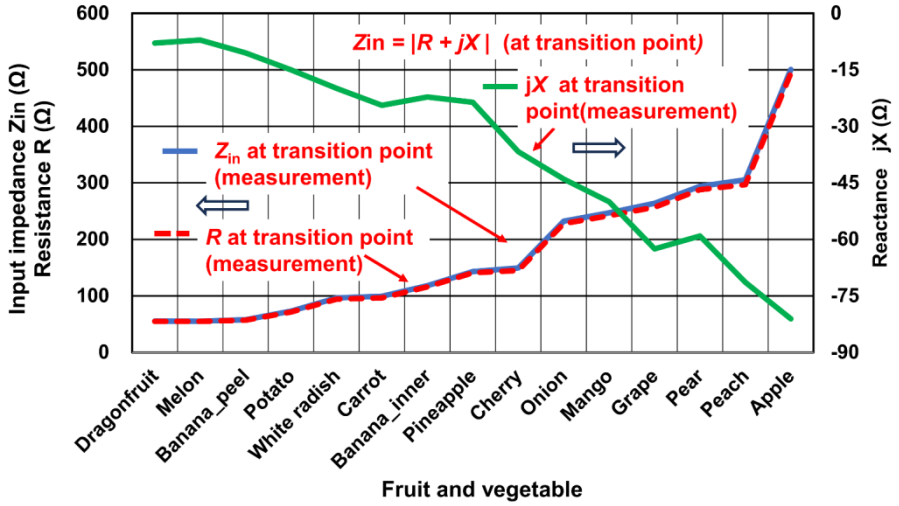

Figure13: Impedance Z_{in}, resistance R, and reactance jX at the transition point of fifteenplants

VIII. VERIFICATION OF THE RELATIONSHIP BETWEEN IMPEDANCE TRANSITION POINTS AND CELL WALLS IN PLANT CELLS

To verify that the impedance Z_{in} transition point in plant cells is related to the cell wall, we finely grated plant samples and filtered them into the liquid portion, which mainly contains vacuoles, from the solid portion, which includes the cell wall. Since plant cells are 100 µm to 200 µm in size, a 20 µm paper filter was used to filter and remove the solid portion after grating, and the S-parameter S_{11} of the remaining liquid was measured. When the impedance Z_{in} values are plotted on the admittance grid of the Smith chart, the transition points and the impedance Z_{in} curve in the low-frequency region disappear, and only the curve along the admittance grid lines appears, as shown in Figure 15. Since the filtered liquid mainly comprises vacuoles, the disappearing transition points in the impedance Z_{in} are related to the removed cell walls.Comparing the changes in the equivalent circuits of the plant cells, as shown in Figure 15, the paths Y_2, Y_3, and Y_4, including the series circuit, are eliminated, and only the path Y_1 remains. Therefore, the path of the series circuit along the impedance grid lines has disappeared.

The vacuole contains ionized substances such as Na^+, Ca^+, K^+, Cl^-, and HPO_4^{2-} and polar molecules such as H_2O. When 100 MHz or less frequency electrical signals are applied, these ions move, rotate, and vibrate. H_2O polar molecules do not contribute to conductance at frequencies below 100 MHz because they respond to high frequencies above several hundred MHz [23]. The filtered liquid contains cell membrane and cytoplasm residues of less than 20 µm in size that are not removed and become electrical resistances. These

resistive components are connected in parallel with C_1 as resistor R_1. The filtered liquid can be considered as an equivalent circuit of a capacitor with complex permittivity, where C_1 and R_1 are related to the real and imaginary parts of the complex permittivity, ε′ and ε″, respectively. The electrical loss factor of the filtered liquid is defined as $\tan\delta = 1/(\omega C_1 R_1) = \varepsilon''/\varepsilon'$.

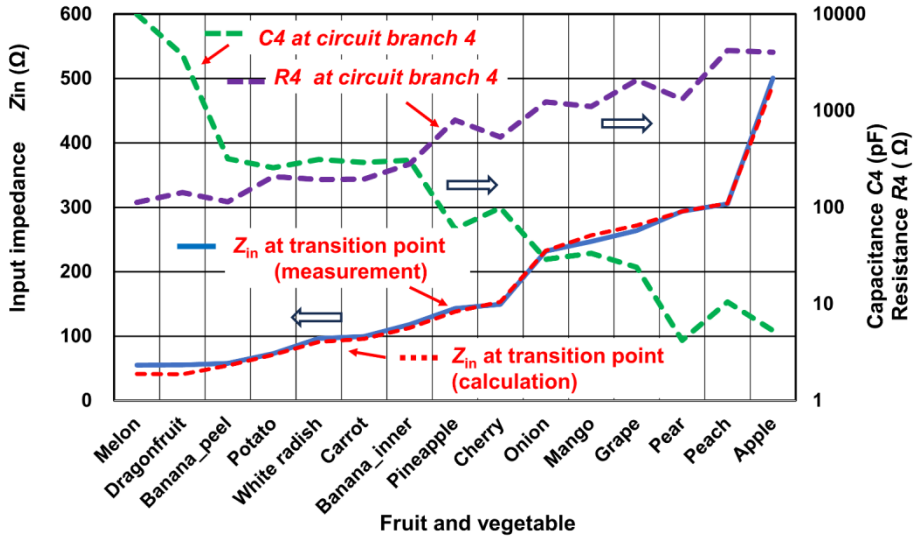

Figure14: Measured and calculated impedance Z_{in} of the equivalent circuit at the transition point of fifteen plants and the values of the circuit elements R_4 and C_4, which indicate the cell wall

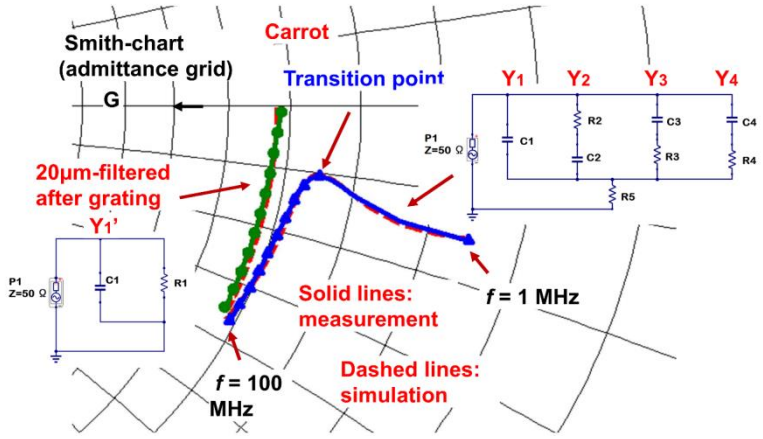

Figure15: Difference between the measured impedance Z_{in} of a plant sample in the untreated state and the Z_{in} after grating and filtering through a 20 μm filter and the equivalent circuit

IX. CONCLUSION

The input impedance Z_{in} calculated from the S-parameter S_{11} measured on the plant sample was plotted on a Smith chart. The transition point is where the reactance jXincreases (|jX| decreases) and then decreases (|jX| increases) with frequency, and in the equivalent circuit, the circuit changes from a series circuit to a parallel circuit. For the input admittance Y_{in}, the susceptance jB decreased to increase at the transition point. Fifteen fruits and vegetables were examined for input impedance Z_{in}, and the frequency at the transition point tended to be lower for fruits and higher for vegetables. The transition point was related to the elements of the series circuit of R_4 and C_4, which represent the cell walls of plant cells. The magnitude of the impedance Z_{in} at the transition point was proportional to R_4, and the frequency of the transition point was proportional to C_4.The sample was grated and filtered through a 20 μm paper filter to remove most of the cell wall to test the hypothesis that the transition point is related to the plant cell wall. After filtration, the impedance Z_{in} of the residual fluid showed

that the transition point disappeared, and the only equivalent circuit was a parallel circuit representing the vacuole. This result indicates that the transition points in the input impedance Z_{in} of plant cells represent the characteristics of the cell wall and depend on the plant variety. It was found that the plant cell characteristics can be analyzed by examining the transition points in the plant impedance.

REFERENCES

[1] A. Fuentes, J. L. Vzquez-Gutierrez, Maria B. Perez-Gago,E. Vonasek, N. Nitin, D. M. Barrett "Application of nonde- structive impedance spectroscopy to determination of the effect of temperatureonpotato microstructureand tex-ture, Journal of Food Engineering, 133, pp.16-22, (2014). doi:10.1016/j.jfoodeng.2014.02.016

[2] D. E. Khaled, N. Novas, J. A. Gazquez, R. M. Garcia, F. Manzano-Agugliaro, "Fruit and Vegetable Quality Assessment via Dielectric Sensing, Sensors, 15, pp.15363-15397, (2015). doi:10.3390/s150715363

[3] X. Zhao, Hong Zhuang, S. Yoon, Y. Dong, W. Wang, andW. Zhao, "Electrical Impedance Spectroscopy for Quality Assessment of Meat, Fish: A Review on Basic Princi- ples, Measurement Methods, and Recent Advances, Hin- dawi Journal of Food Quality, 6370739, 16 pages, (2017). doi:10.1155/2017/6370739

[4] B. M. Aboalnaga, L. A. Said, A. H. Madian, A. S. Elwakil,A. G. Radwan, "Cole Bio-Impedance Model Variations in Daucus Carota Sativus Under Heating and Freezing Conditions, IEEE Openaccess, vol.7, pp.113254-113263, (2019). doi:10.1109/access.2019.2934322

[5] M. A.Trandel, S. Johanningsmeier, J. Schultheis, C. Gunter and P. Perkins-Veazie, " Cell Wall Polysaccharide Composition of Grafted Liberty Watermelon With Reduced In- cidence of Hollow Heart Defect , Front. Plant Sci., vol.12, (2021). doi:10.3389/fpls.2021.623723

[6] M. V. Haeverbeke, B. D. Baets, M. Stock, "Plant impedance spectroscopy: a review of modeling approaches and applications , Frontiers in Plant Science, pp.1-17, 31 July (2023). doi:10.3389/fpls.2023.1187573

[7] K. Chinen, S. Nakamoto, I. Kinjo, "RF Analysis of Fruit and Vegetables using Equivalent Circuits Deduced from S-parameters, International Journal of Electrical and Com- puter Engineering Research, vol. 3, no.2, pp.18-24, (2023). doi:10.53375/ijecer.2023.342

[8] M. I. Hussain, A. El-Keblawy, N. Akhtar, A. S. Elwakil, " Electrical Impedance Spectroscopy in Plant Biology, Sustainable Agriculture Reviews vol.52, pp. 395416, (2021). doi:10.1007/978-3-030-73245-5-12

[9] Menna Mohsen, Lobna A. Said, Ahmed H. Madian, AhmedG. Radwan, Ahmed S. Elwakil, "Fractional-Order Bio- Impedance Modeling for Interdisciplinary Applications: A Review, IEEE access, vol.9, pp.33158-33168, 2021. doi:10.1109/access.2021.3059963

[10] K. Kadan-Jamala, M. Sophocleousb, A. Jogc, D. Desaganic,O. Teig-Sussholzd, J. Georgioub, A. Avni, Y. Shacham- Diamand, "Electrical impedance spectroscopy of plant cells in aqueous buffer media over a wide frequency range of 4 Hz to 20 GHz , Method Article, vol. 8, 101185, (2021). doi:10.1016/j. mex.2020.101185

[11] https://qucsstudio.de/

[12] https://www.awr.com

[13] H. Ando, T. Imaizumi, "Changes in electrical properties and void distribution of mung bean sprouts during hot water heating, Food Science and Technology Research, 27 (2), 311318, (2021). doi:10.3136/fstr.27.311

[14] K.W. Waldron, M.L. Parker, and A.C. Smith, "Plant Cell Walls and Food Quality Introduction , Comprehensive Reviews in Food Science and Food Safety, Insti- tute of Food Technologists, 20 Nov. pp.128-146, (2006). doi:10.1111/j.1541-4337.2003.tb00019.x

[15] C. Holland, P. Ryden, C. H. Edwards, M. M. L. Grundy, "Plant Cell Walls: Impact on Nutrient Bio- accessibility and Digestibility, Foods, 9, 201, pp.1-16, (2020). doi:10.3390/foods9020201

[16] R. Prakash, A. S. Ninan, R. G. Atkinson, R. J. Schaffer, I.C. Hallett, R. Schroder, "Fruit From Two Kiwifruit Genotypes with Contrasting Softening Rates Show Differences in the Xyloglucan and Pectin Domains of the Cell Wall, Christina G. Fullerton, Front. Plant Sci., vol.11, (2020). doi:10.3389/fpls.2020.00964

[17] K. Jia, W. Wang, Q. Zhang, W. Jia, "Cell Wall Integrity Signaling in Fruit Ripening , Int. J. Mol. Sci., 24, 4054, (2023). doi:10.3390/ijms24044054

[18] Q. Yin, W. Qin, Z. Zhou, A. M. Wu, W. Deng, Z. Li, W. Shan, J. Chen, J. Kuang, W. Lu, "Banana MaNAC1 activates secondary cell wall cellulose biosynthesis to enhance chilling resistance in fruit , Plant Biotechnology Journal 22, pp. 413-426, (2024). doi:10.1111/pbi.14195

[19] S. Ehosioke, F. Nguyen, S. R, T. Kremer, E. Placencia- Gomez, J. A. Huisman, A. Kemna, M. Javaux, S. Garre, "Sensing the electrical properties of roots: A review , Vadose Zone Journal, vol.19, issue 1, e20082. (2020). doi:10.1002/vzj2.20082

[20] M. Szymanska-Chargot, M. Chylinska, P. M. Pieczyweka,P. Rosch, M. Schmitt, J. Popp, A. Zdunek, " Raman imaging of changes in the polysaccharides distribution in the cell wall during apple fruit development and senescence, Planta, 243, pp. 935945, (2016). doi:10.1007/s00425-015-2456-4

[21] J. C. Nouaze, J. H. Kim, G. R. Jeon, J. H. Kim, "Monitor- ing of Indoor Farming of Lettuce Leaves for 16 Hours Using Electrical Impedance Spectroscopy(EIS) and Double-Shell Model (DSM), Sensors, vol. 22, pp.9671, (2022). doi:10.3390/s22249671

[22] S. Lin, T. Lin, C. K. M. Yee, J. Chen, Y. W. M. K. Nalla,D. W. Barchenger, " Selection of Pollen Traits Under High Temperature Stress in Pepper , Hortscience 57(2):181190, (2022). doi:10.21273/hortsci16258-21

[23] K. Chinen, S. Nakamoto, I. Kinjo, " Two-port Equivalent Circuit Deduced from S-parameter Measurements of NaCl Solutions," IETE Journal of Research IF 1.877, pp.1- 9, (2022). doi:10.53375/ijecer.2023.342